

# Partial Imaginary Precursor Cancelling in DFE For BPSK and GMSK Modulations

DAN RAPHAELI, AMIT STARK

Department of Electrical Engineering - Systems, Tel Aviv University, Israel.

June 17, 2001

**Abstract.** This paper examines the effect of partial imaginary precursor cancelling on the performance of a system which uses a DFE and employs a one dimensional modulation. As opposed to QAM, BPSK or GMSK (after proper manipulations) require minimization of the mean square (MS) of the error real part only. Therefore, a lower MSE is achieved if the DFE coefficients are computed taking this fact into account, by trying to minimize as few imaginary precursors as possible. However, this introduces a delay by the imaginary part of the feedback filter (FBF) which is no longer causal.

In this paper we investigate the influence of the length of imaginary precursor cancelling on system performance, and its effect on carrier phase tracking. The equations for the computation of the DFE coefficients for none or partially cancelled imaginary precursors are derived and performance on GMSK channels is presented.

## I. INTRODUCTION

Decision feedback equalization (DFE) is used to mitigate to effects of intersymbol interference in multipath fading channels. A common application of DFE is wireless local area network (LAN) modems [1]. The computation of the DFE coefficients can be performed using an adaptation algorithm such as LMS which is easy to implement but requires a long training sequence for convergence [2]-[3]. Another approach is to estimate the channel impulse response using a short preamble sequence (50-100 bits) from which the DFE taps are calculated [4], [5].

Offset quaternary phase shift keying (OQPSK) or a linear approximated Gaussian minimum shift keying (GMSK) are two equivalent modulation schemes which are widely used in wireless modems [4]. Using GMSK modulation and DFE equalization has been widely investigated, since DFE significantly reduces the ISI introduced by the pre-modulation Gaussian filter used in GMSK modulation [6]-[7]. It is used in the European GSM system and the HIPER-LAN standard [8]-[9]. OQPSK can be made equivalent to binary phase shift keying (BPSK) modulation with the addition of differential encoding in the transmitter and a multiplier by  $j^{-i}$  in the receiver before the equalizer. The channel that is seen by the equalizer in this case is  $h_i = f_i j^{-i}$ . The advantage of adjusting the equations to the BPSK case is that the MSE is minimized in the real dimension only

which results in improved performance in comparison to an equalizer that needlessly minimizes both the real and imaginary MSE. Using BPSK modulation and DFE has also been investigated [10]; however, closed form DFE equations for real and partial imaginary MSE minimization for improved performance have not been derived.

The DFE equations for QPSK modulation are well known [11]. A compact formulation is found in [12]. We present here the derivation for the BPSK case. Since minimization of the MSE is performed in the real dimension only, the unminimized imaginary precursors no longer have negligible magnitudes, thus affecting the performances of a carrier tracking phase locked loop (PLL) and the adaptation of the equalizer coefficients \*. The PLL driving signal which ideally is the received symbol at  $k = 0$  (without ISI) with its phase rotated, now includes also these precursors, which are considered to be noise and increase the error in phase estimation. These unminimized imaginary precursors are cancelled by the feedback filter (FBF) which is no longer causal, thus introducing a delay in the system. To decrease this delay we can include only some of the imaginary precursors in the MSE minimization. This addition causes performance degradation since now the equalizer has to minimize imaginary precursors as well, and min-

---

\* Although an adaptive algorithm like the LMS can adapt using the real error only, convergence is much improved if the imaginary part is used as well.

imization of the real part, which is used by the decision component, is not optimal. Therefore, a trade-off exists when partially cancelling the imaginary precursors: addition of minimized precursors results in performance degradation but less delay is introduced.

After performing minimization on a given length of imaginary precursors we can further decrease the delay by neglecting some of the unminimized imaginary precursors and not cancel them by the FBF. By doing this we increase the magnitude of the precursors and thus the error in the driving signal of the PLL. Thus, there are two ways to reduce the delay in the system: minimizing only some of the imaginary precursors and then cancelling only some of the remaining unminimized ones by the FBF. Both of these methods introduce errors in the system, and for best performance we must find an optimal working point in which the delay and the errors are as minimal as possible.

In this paper we examine system performance and determine the effect of partial imaginary precursor cancelling. We introduce the system model and derive closed form equations for none or partially cancelled imaginary precursors. We present the two methods used for reducing the delay in the system and the errors that they introduce. Then, simulations are performed for a DFE with 23 (FBF) and 8 (FFF) taps on GMSK channels with rms delay spread of  $150n_s$ . We show that 2dB improvement in system performance is achieved on a specific channel (for  $E_b/N_0 = 10dB$ ), and a 1 dB improvement (for the same  $E_b/N_0$ ) is achieved on the average, by neglecting only one imaginary precursor in the minimization. Increasing the  $E_b/N_0$  improves system performance even better. At the expense of an additional small error, minimization can be done on less imaginary precursors and then neglecting most of the unminimized ones, leaving only one unminimized imaginary precursor to be cancelled by the feedback filter (FBF). By doing this we achieve an optimal working point at which the delay and the errors are minimal.

## II. SYSTEM MODEL

Let us assume a linearized GMSK modulator at the transmitter. GMSK modulation is created by passing BPSK modulated data in baseband ( $x_n = \pm 1$ ) through a  $j^n$  multiplier and a pulse shaping filter  $h_G(t)$

$$x(t) = \sum_{n=-\infty}^{\infty} x_n j^n h_G(t - nT), \quad (1)$$

where T is the symbol length. The signal then enters a channel  $f(t)$  with additive noise  $n_0(t)$  after which we place an anti-aliasing filter  $h_{aa}(t)$

$$r(t) = x(t) * f(t) * h_{aa}(t) + n_0(t) * h_{aa}(t) =$$

$$\sum_{n=-\infty}^{\infty} x_n j^n q(t - nT) + w(t), \quad (2)$$

where  $q(t) = x(t) * f(t) * h_{aa}(t)$ ,  $w(t) = n_0(t) * h_{aa}(t)$  and \* denotes convolution. In the receiver we sample the signal and multiply it by  $j^{-k}$  to convert it back to BPSK modulated signal

$$c_k = \sum_{n=-\infty}^{\infty} x_n j^{n-k} q((k - n)T) + v_k = \sum_{n=-\infty}^{\infty} x_n u_{k-n} + v_k, \quad (3)$$

as can be seen in Figure 1.  $c_k$  and  $v_k$  are the sampled and derotated versions of  $r(t)$  and  $w(t)$ , respectively.

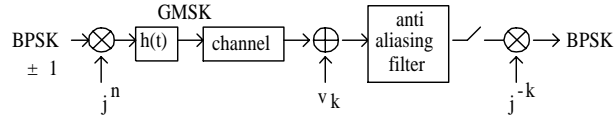


Figure 1: System model.

The system can be equally modelled using BPSK only as given by

$$z_i = \sum_{n=-\infty}^{\infty} x_n h_{i-n} + n_i. \quad (4)$$

The results are independent of the modulation level, so any PAM system can also be used. When doing the conversion depicted above, any QPSK or OQAM can equivalently be used. Thus, without loss of generality, we can assume using a BPSK modulation system.

Denote the equivalent channel impulse response by  $\mathbf{h}$  with components  $h_l, l = 0, \dots, \nu$  and the feedforward filter (FFF) of length  $N_f$  by  $\mathbf{w}$  with components  $w_l, l = 1 - N_f, \dots, 0$ . Let

$$g_k = \sum_{l=1-N_f}^0 w_l h_{k-l}. \quad (5)$$

We denote

$$b_m = \begin{cases} j\text{Im}\{g_m\} & m < 1 \\ g_m & m \geq 1 \end{cases} \quad (6)$$

and define

$$FBF_r \equiv \text{Re}\{b\}$$

$$FBF_i \equiv \text{Im}\{b\}. \quad (7)$$

In the QPSK case the FBF is of length  $N_b$  with components  $b_l, l = 1, \dots, N_b$  ( $N_b = \nu$ ). The imaginary FBF

( $FBF_i$ ) is causal and thus no delay is introduced. In the BPSK case, the  $FBF_i$  is used to cancel the unminimized imaginary precursors as well. Therefore the  $FBF_i$  is of length  $N_b + N_f$  with components  $b_l, l = 1 - N_f, \dots, N_b$  (the  $FBF_r$  is still of length  $\nu$ ). The  $FBF_i$  is no longer causal, and it has  $N_f - 1$  anticausal taps.

In the partial imaginary precursor cancelling case we perform minimization only on some of the imaginary precursors in order to decrease the delay that is created in the system. Define  $-L$  as the index of the last imaginary precursor on which minimization is done, which results in  $L - 1$  unminimized imaginary precursors. As in the BPSK case, the  $FBF_i$  is used to cancel the unminimized imaginary precursors as well. Therefore the  $FBF_i$  is of length  $N_b + L$  (for  $L \geq 1$ ) with components  $b_l, l = -L + 1, \dots, N_b$ . The  $FBF_i$  is not causal, and it has  $L - 1$  anticausal taps.

In order to further reduce the delay created in the system, we can neglect some unminimized imaginary precursors and not cancel them by the  $FBF_i$ . Let  $d$  be the number of these neglected precursors. The resulting  $FBF_i$  is of length  $N_b + L - d$  with components  $b_l, l = -(L - d) + 1, \dots, N_b$ . Therefore, the delay (number of anticausal taps) has been reduced by  $d$ , as can be seen in Figure 2.

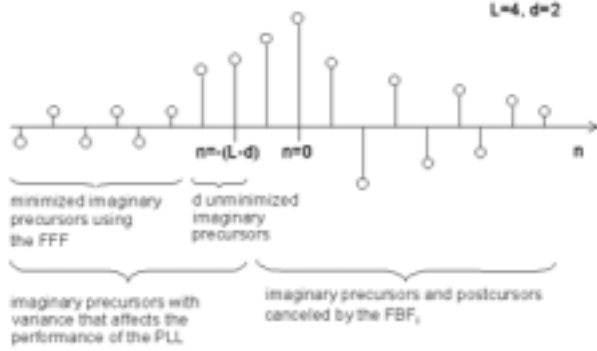


Figure 2: The channel after the FFF showing which imaginary precursors are cancelled by the  $FBF_i$  and which are affecting the PLL for  $L=4, d=2$ .

Carrier phase tracking is done using a first order digital PLL which difference equation is given by

$$\hat{\theta}_{i+1} = \hat{\theta}_i + K \Delta \theta_i, \quad (8)$$

where  $K$  is the loop gain.  $\Delta \theta_i$  is calculated using

$$\Delta \theta_i = \text{Im} \left\{ \frac{y_i e^{-j\hat{\theta}_i} - \sum_{k=1}^{N_b} \hat{x}_{i-k} g_k - \sum_{k=-1}^{-L-d} \hat{x}_{i-k} b_k}{g_0} \hat{x}_i \right\}, \quad (9)$$

where  $y_i = z_i * w_i$ , i.e. the symbol received after the FFF.

We define the PLL driving signal as the numerator in equation (9). Ideally this signal includes only the symbol at  $k = 0$  which is phase rotated. Any precursor not cancelled by the FBF is considered as noise which increases the MSE, thus affecting the phase estimation. Clearly, unminimized imaginary precursors not cancelled by the  $FBF_i$  increase the MSE more than minimized ones. For best performance we want  $L - d$  to be as large as possible, so that more imaginary precursors are not minimized but cancelled by the  $FBF_i$ , and minimization of the real part is optimal. Hence we achieve good performance in symbol detection and carrier phase tracking, at the expense of a larger delay introduced in the system.

Assuming a random walk frequency phase which model is given by  $\theta_i = \theta_{i-1} + \vartheta_i$  where  $\vartheta_i$  is AWGN, and using equations (8), (9) and  $e_i = \theta_i - \hat{\theta}_i$ , where  $e_i$  is the estimation error, it can be shown that the residual phase jitter is given by

$$\sigma_i^2 = \frac{\frac{k^2}{g_0^2} \sum_{1-N_f}^{-(L-d+1)} (g_k^i)^2 + \sigma_\vartheta^2 + \frac{k^2}{g_0^2} \frac{\sigma_n^2}{2}}{2K - \frac{k^2}{g_0^2} \sum_{1-N_f}^{N_b} (g_k^i)^2}, \quad (10)$$

where  $\sigma_i^2 = E[e_i^2]$ ,  $\sigma_n^2 = E[n_i^2]$ ,  $\sigma_\vartheta^2 = E[\vartheta_i^2]$ , and  $(\cdot)^r, (\cdot)^i$  denote the real and imaginary parts, respectively. It was assumed that the detected symbols are correct. As can be seen from equation (10), the larger  $L - d$  is, the smaller the residual phase jitter, as previously explained (the details of the derivation will be given in a later article).

We present in Figure 3 a combined PLL and DFE configuration in which decision is done based on the real output of the FBF, while the received symbol, detected symbol and both the real and imaginary FBF outputs are used by the phase detector of a PLL for carrier phase acquisition, as given by equation (8).



Figure 3: DFE configuration.

We assume that the FBF perfectly cancels the postcursor ISI within its span and the FFF minimizes the MSE resulting from the precursors and the noise.

### III. COMPUTATION OF THE DFE COEFFICIENTS

#### A. QPSK MODULATION

We assume symbol spaced equalizer (the equations are easily extended to fractionally spaced equalizers). The data symbols are i.i.d. and independent of the noise samples. We also assume that the FBF is fed by correct decisions of the detected symbols and that the residual precursors have a Gaussian distribution. Following the derivation in [12] we get the solution for  $\mathbf{w}$  for the QPSK case which minimizes the MSE. The equation is

$$\mathbf{w} = \mathbf{\Omega}^{-1} \cdot \mathbf{p}, \quad (11)$$

where  $\mathbf{\Omega}$  is a square matrix of dimension  $N_f$ ,

$$\Omega_{i,j} = \bar{\Omega}_{i,j} + R_n((i-j)T) = \sum_{n=1-N_f}^0 h_{n-i}^* h_{n-j} + R_n((i-j)T), \quad (12)$$

where  $n = 0$  is the decision point,  $R_n(\tau)$  is the autocorrelation function of the additive noise and  $\mathbf{p}$  is a vector of size  $N_f$  where  $p_i = h_{-i}^*$ .

The variance of the noise after passing through the FFF and FBF is given by

$$\sigma_{\text{noise}}^2 = E \left[ \left| \sum_{l=1-N_f}^0 w_l n_{k-l} \right|^2 \right] = \sum_{l=1-N_f}^0 \sum_{m=1-N_f}^0 w_l^* w_m R_{l-m}, \quad (13)$$

where  $R_{l-m} = E[n_{k-m} n_{k-l}^*] = R_n((l-m)T)$ .

We can write the MSE after the FFF and FBF as the sum of ISI and noise components (assuming the FBF cancels the effect of the postcursors)

$$\varepsilon_c^2 = \sum_{k=1-N_f}^{-1} |g_k|^2 + |1 - g_0|^2 + \sigma_{\text{noise}}^2 = \sum_{k=1-N_f}^0 |g_k|^2 - 2\text{Re}(g_0) + 1 + \sigma_{\text{noise}}^2. \quad (14)$$

It can be shown that

$$\varepsilon_c^2 = \mathbf{w}^\dagger \mathbf{\Omega} \mathbf{w} - 2\text{Re}\{\mathbf{w}^\dagger \cdot \mathbf{p}\} + 1, \quad (15)$$

where  $'\dagger'$  is the conjugate Hermitian operator.

#### B. BPSK MODULATION

Define  $\tilde{w}_{2k} = \text{Re}(w_k)$ ,  $\tilde{w}_{2k+1} = \text{Im}(w_k)$ ,  $\tilde{p}_{2k} = \text{Re}(p_k)$  and  $\tilde{p}_{2k+1} = \text{Im}(p_k)$ .

The MSE is now calculated by taking the real part of  $g_k$  (for a one dimensional constellation) in equation (14) and using half the variance of the noise

$$\varepsilon_r^2 = \sum_{k=1-N_f}^0 \left( \sum_{l=1-N_f}^0 \text{Re}\{w_l h_{k-l}\} \right)^2 - 2\text{Re} \left( \sum_{l=1-N_f}^0 w_l h_{-l} \right) + 1 + \frac{\sigma_{\text{noise}}^2}{2} \quad (16)$$

and by a similar derivation we get

$$\varepsilon_r^2 = \tilde{\mathbf{w}}^T \tilde{\mathbf{\Omega}}^r \tilde{\mathbf{w}} - 2(\tilde{\mathbf{w}}^T \cdot \tilde{\mathbf{p}}) + 1. \quad (17)$$

where  $\tilde{\mathbf{\Omega}}^r$  is defined in the appendix. Following the derivation in the appendix, the equation for finding the coefficients for the BPSK case becomes

$$\tilde{\mathbf{w}} = (\tilde{\mathbf{\Omega}}^r)^{-1} \tilde{\mathbf{p}}, \quad (18)$$

where we assume (for now) a fully BPSK solution, i.e. minimization is done on the real precursors only and  $\tilde{\mathbf{\Omega}} = \tilde{\mathbf{\Omega}}^r$ . This assumption will be relaxed in the next section, where we will demonstrate partial imaginary precursor cancelling.

The SNR is given by

$$\text{SNR} = \frac{\text{Re}^2(g_0)}{\sum_{k=1-N_f}^{-1} \text{Re}^2(g_k) + \frac{\sigma_{\text{noise}}^2}{2}} \quad (19)$$

Using the assumption that the residual ISI has a Gaussian distribution and that the decisions feedback are correct  $\hat{x}_i = x_i$ , the BER is calculated using

$$\text{BER} = Q(\sqrt{\text{SNR}}) \quad (20)$$

#### C. VARIABLE LENGTH IMAGINARY PRECURSOR CANCELLING

So far we have assumed that MSE minimization is done on the real precursors only. In order to perform the minimization on part of the imaginary precursors as well, we need to change the indexes in the summations in the definitions of  $\tilde{\mathbf{\Omega}}^i$  to include only those precursors we want to minimize. Rewriting the definitions of  $\tilde{\mathbf{\Omega}}^i \mathbf{p}^i$  as given in the appendix,

$$\begin{aligned} \tilde{\Omega}_{2l,2m}^i &= \sum_{k=1-N_f}^{-L} h_{k-l}^i h_{k-m}^i + \frac{1}{2} R_{l-m}^r \\ \tilde{\Omega}_{2l,2m+1}^i &= \sum_{k=1-N_f}^{-L} h_{k-l}^i h_{k-m}^r - \frac{1}{2} R_{l-m}^i \\ \tilde{\Omega}_{2l+1,2m}^i &= \sum_{k=1-N_f}^{-L} h_{k-l}^r h_{k-m}^i + \frac{1}{2} R_{l-m}^i \end{aligned}$$

$$\tilde{\Omega} p_{2l+1,2m+1}^i = \sum_{k=1-N_f}^{-L} h_{k-l}^r h_{k-m}^r + \frac{1}{2} R_{l-m}^r, \quad (21)$$

where  $L \in 0, \dots, N_f$ .  $-L$  is the index of the last imaginary precursor included in the minimization.  $n = 0$  is the decision point and thus choosing  $L = 0$  gives the fully complex solution, where we minimize all imaginary precursors (as in the QPSK case), while choosing  $L = N_f$  gives the full solution for BPSK, where we do not include any imaginary precursor in MSE minimization. The larger  $L$  is, the less imaginary precursors are included in the minimization, which results in better system performance but more delay is introduced in the system.

Following the derivation in the appendix (using  $\beta = 1$ ) we arrive at the following equation for the DFE coefficients

$$\tilde{\mathbf{w}} = \tilde{\Omega}^{-1} \cdot \tilde{\mathbf{p}} = (\tilde{\Omega}^r + \tilde{\Omega} p^i)^{-1} \tilde{\mathbf{p}}. \quad (22)$$

After making this change in  $\tilde{\mathbf{w}}$ , the MSE, SNR and BER are calculated using equations (17), (19) and (20), respectively (in equation (17) we substitute  $\tilde{\Omega}$  for  $\Omega^r$ ).

We compare the signal after passing through the FFF in three different cases (where  $N_f = 8$ ): the first is for only one imaginary precursor minimized ( $L = 7$ ), the second is for partially cancelled precursors ( $L = 3$ ), and the third is the fully complex case (where all the imaginary precursors are minimized and  $L = 0$ ), as can be seen in Figure 4, where we chose an arbitrary channel as an example. The amount of imaginary precursors cancelled is an evidence to the loss in performance caused by needlessly performing this minimization.

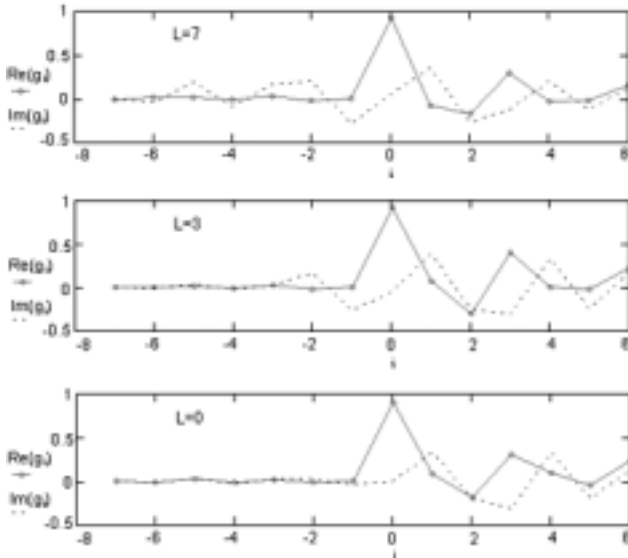


Figure 4: The signal after passing through the FFF for  $L=7, L=3$ , and  $L=0$ .

In addition to the MSE for the real part, there exists

an imaginary MSE that has an effect on the performance of the PLL. As previously mentioned, it is caused by the minimized imaginary precursors and the noise and is given by:

$$\varepsilon_i^2 = \sum_{k=1-N_f}^{-L} (\text{Im}\{g_k\})^2 + \frac{\sigma_{\text{noise}}^2}{2} \quad (23)$$

After choosing a value for the parameter  $L$ , we have  $L - 1$  unminimized imaginary precursors. Choosing a large value for  $L$  results in better system performance, i.e. smaller  $\varepsilon_r^2$  and  $\varepsilon_i^2$ , but more delay is caused by the  $FFFi$ . In order to decrease this delay we can discard some of these unminimized imaginary precursors and not cancel them by the  $FFFi$ . However, by doing this we cause a larger imaginary MSE ( $\varepsilon_i^2$ ). Therefore, a trade-off exists between a smaller delay and a larger  $\varepsilon_i^2$  when discarding some of the unminimized imaginary precursors. Denote by  $d$  the number of discarded unminimized imaginary precursors. The resulting delay is now  $L - 1 - d$  and the imaginary MSE is given by

$$\varepsilon_i^2 = \sum_{k=1-N_f}^{-(L-d)} (\text{Im}\{g_k\})^2 + \frac{\sigma_{\text{noise}}^2}{2}. \quad (24)$$

Using the equation for  $\tilde{\mathbf{w}}$  we can write

$$\begin{aligned} \text{Im}\{g_0\} &= \text{Im}\left\{ \sum_{l=1-N_f}^0 w_l h_{-l} \right\} = \text{Im}\{ \tilde{\mathbf{p}}_1^T \cdot \tilde{\mathbf{w}} \} = \\ &= \text{Im}\{ \tilde{\mathbf{p}}_1^T \cdot \tilde{\Omega}^{-1} \cdot \tilde{\mathbf{p}} \}, \end{aligned} \quad (25)$$

where  $\tilde{p}_{1,2k} = -\text{Im}(p_k)$  and  $\tilde{p}_{1,2k+1} = \text{Re}(p_k)$ . Using symmetries in the definitions of  $\tilde{\Omega}$  from the appendix, we can write

$$\tilde{\Omega} = \mathbf{A} + \mathbf{B} + \mathbf{A}^T \quad (26)$$

where  $\mathbf{A}$  is an upper triangular block matrix with symmetric blocks of size  $2 \times 2$  where the two diagonal elements of each block are equal, and  $\mathbf{B}$  is a diagonal block matrix with diagonal blocks of size  $2 \times 2$  that have equal elements. Since  $\tilde{\Omega}$  can be written in this form, it can be shown that  $\tilde{\Omega}^{-1}$  has a similar decomposition. Furthermore, it can be shown that a matrix of this sort, when multiplied by two vectors such as  $\tilde{\mathbf{p}}$  and  $\tilde{\mathbf{p}}_1$  as in equation (25), yields a zero result. Therefore

$$\text{Im}\{g_0\} = 0. \quad (27)$$

Since the imaginary part of  $g$  at the decision time is always zero, the results obtained for  $L = 0$  and  $L = 1$  will be equal, because no effort is required by the equalizer to minimize this sample.

IV. SIMULATION RESULTS

We used GMSK modulation over Rayleigh fading channels with exponential decay power-delay profile and RMS delay spread of  $150ns$ . The impulse responses are estimated using preamble sequences, and the parameters are as given by the GSM standard where  $BT = 0.3$ . The anti-aliasing filter in the receiver is chosen to match the pulse shape filter in the transmitter. The channels have 23 taps and the DFE filters' lengths are  $N_b = 23$  and  $N_f = 8$  (the equalizer is symbol spaced). By virtue of the MMSE criterion, the imaginary part of  $g$  at the decision time is zero, as proved in the previous section. Therefore the graphs start with  $L$  taking the value of 1. The  $E_b/N_0$  used was 10dB, where  $E_b$  is the energy per transmitted bit and  $N_0$  is the two-sided power spectral density of the AWGN (it also equals half the SNR).

The SNR and BER were calculated analytically using equations (19) and (20), respectively, where we assumed that the decisions fed back are correct. Simulations were performed on one specific channel which showed better improvements relative to the others, and on 1000 channels where the average performance was calculated. Results for the BER and SNR as a function of the length of imaginary precursors for a single channel are shown in Figures 5 and 6. BER as a function of  $E_b/N_0$  with  $L$  as a parameter for a single channel and for the average are shown in Figures 7 and 8. BER cumulative distribution function (the percentage of channels for a given BER, as in [2]) with  $L$  as a parameter for the average is shown in Figure 9. As can be seen from Figures 5,6 and 7, the major improvement (approx. 2dB for  $E_b/N_0 = 10dB$ ) occurred when we left out one precursor ( $L = 2$ ) while minimizing the MSE, which does not cause a major delay in the system. Similarly, an average of 1dB (for  $E_b/N_0 = 10dB$ ) improvement was achieved by neglecting the first imaginary precursor in the 1000 channels checked, as can be seen from Figures 8 and 9. Increasing the  $E_b/N_0$  improves the performance even further.

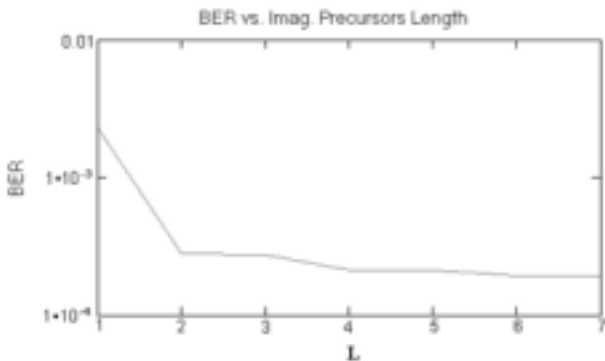


Figure 5: BER vs. imaginary precursors length - single channel.

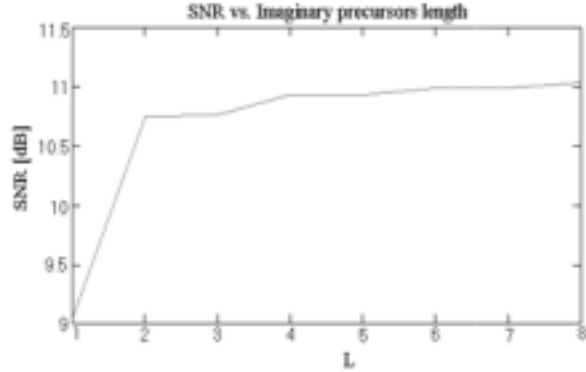


Figure 6: SNR vs. imaginary precursors length - single channel.

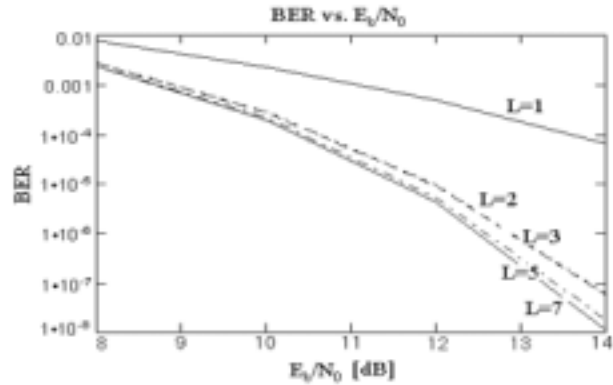


Figure 7: BER vs.  $E_b/N_0$  single channel ( $L$  is a parameter).

In order to find the number of unminimized imaginary precursors needed for near optimum performance, which we defined as 0.5dB below the maximum SNR achieved by a fully BPSK solution, we performed a simulation on the same channels, and the results are presented in Figure 10. As we can see, in the majority of the channels (83%), only one unminimized imaginary precursor is needed for near optimum performance.

We also calculated, using equation (24), the imaginary MSE that affects the performance of the PLL (average on 1000 channels). This MSE resulted from the minimized imaginary precursors, the noise, and some of the unminimized precursors that we did not cancel by the  $FBF_i$ , for the purpose of decreasing the delay without affecting  $\varepsilon_r^2$ . As can be seen in Figure 11, small  $\varepsilon_i^2$  can be obtained as long as we keep  $d \leq L - 2$ . Therefore we can discard up to  $L - 2$  (for  $L \geq 2$ ) unminimized imaginary precursors and not cancel them by the  $FBF_i$  while not causing a large imaginary MSE. Therefore, for a given length of minimized imaginary precursors, we can discard  $L - 2$  of the unminimized imaginary precursors, leaving only one unminimized imaginary precursor to be cancelled by the  $FBF_i$ , at the expense of a relatively small  $\varepsilon_i^2$ . This results in a small delay and good system performance. A

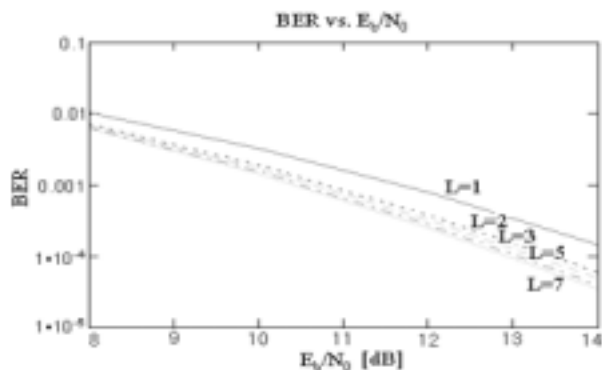


Figure 8: BER vs.  $E_b/N_0$  average on 1000 channels ( $L$  is a parameter).

joint DFE and PLL simulation will be carried out in a later article, where we will also investigate different system configurations and phase estimation procedures.

As an example, consider  $L = 5$ . The last sample included in the minimization is  $n = -5$  and thus we have 3 minimized imaginary precursors and 4 unminimized ones, and the delay is 4 symbols long since the  $FBF_i$  must cancel these precursors. We have performed minimization on some of the imaginary precursors, which is not optimal, and thus we increased  $\varepsilon_r^2$ . The error in the signal that feeds the PLL is caused by the 3 minimized imaginary precursors and the noise, and is given by  $\varepsilon_i^2$ . In order to minimize the delay and not cause a large increase in  $\varepsilon_i^2$  we discard  $L - 2 = 3$  unminimized imaginary precursors. The  $FBF_i$  has only one unminimized precursor to cancel and the resulting delay is now only one symbol long. This operation does not change  $\varepsilon_r^2$ , but  $\varepsilon_i^2$  is now larger due to the 3 discarded unminimized precursors.

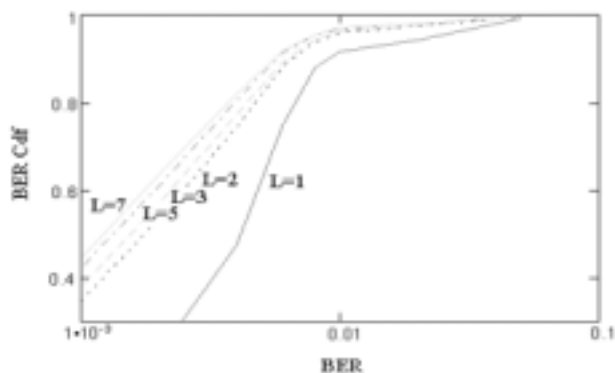


Figure 9: BER Cdf - average on 1000 channels ( $L$  is a parameter).

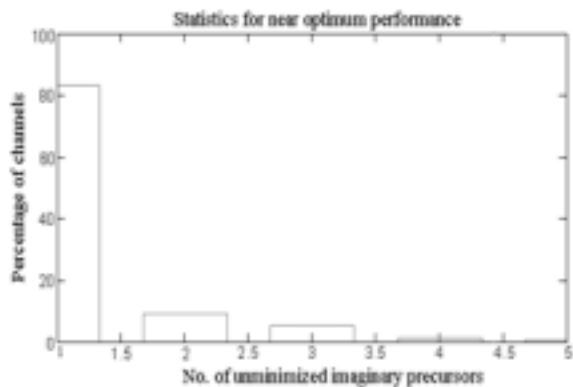


Figure 10: Percentage of channels for near optimum performance (0.5dB less than optimum performance) vs. no. of unminimized imaginary precursors.

## V. CONCLUSIONS

In this paper we derived a closed form solution for the decision feedback equalizer coefficients for none or partially cancelled imaginary precursors. We have demonstrated that when using one dimensional modulations (BPSK or GMSK), system performance is much improved by adjusting the DFE equations to minimize the MS of the error real part only. However, the unminimized imaginary precursors cause a delay in the system and also affect the performance of a carrier phase tracking loop. This trade-off between performance and delay was investigated and simulations were performed on a (8,23) DFE and GMSK channels with RMS delay spread of 150<sub>ns</sub>. We have shown that considerable improvement is achieved by minimizing as few imaginary precursors as possible, then discarding most of the remaining unminimized ones, leaving only one unminimized precursor that is cancelled by the  $FBF_i$ . This introduces only minimal delay in the system.

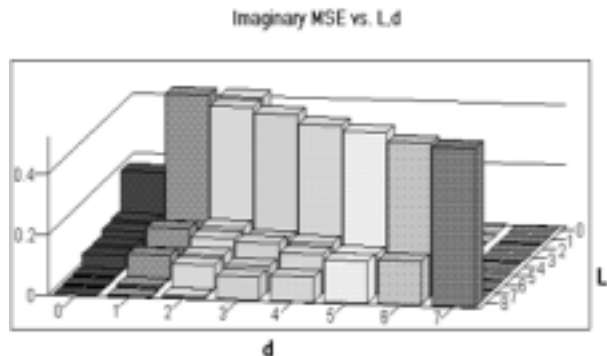


Figure 11: Imaginary MSE vs.  $L, d$  - average on 1000 channels.

## APPENDIX

Let us look at the complex MSE using equation (14)

$$\varepsilon_c^2 = \sum_{k=1-N_f}^0 |g_k|^2 + \sigma_{\text{noise}}^2 - 2\text{Re}(g_0) + 1. \quad (28)$$

Rewriting the first two terms gives

$$\begin{aligned} & \sum_{k=1-N_f}^0 \left| \sum_{l=1-N_f}^0 w_l h_{k-l} \right|^2 + E \left[ \left| \sum_{l=1-N_f}^0 w_l n_{k-l} \right|^2 \right] = \\ & \sum_{k=1-N_f}^0 \left\{ \left[ \text{Re} \left( \sum_{l=1-N_f}^0 w_l h_{k-l} \right) \right]^2 \right. \\ & \left. + \left[ \text{Im} \left( \sum_{l=1-N_f}^0 w_l h_{k-l} \right) \right]^2 \right\} \\ & + E \left\{ \left[ \text{Re} \left( \sum_{l=1-N_f}^0 w_l n_{k-l} \right) \right]^2 \right. \\ & \left. + \left[ \text{Im} \left( \sum_{l=1-N_f}^0 w_l n_{k-l} \right) \right]^2 \right\} \end{aligned} \quad (29)$$

Continuing the derivation for the real part contribution only

$$\begin{aligned} & \sum_{k=1-N_f}^0 \left\{ \text{Re} \left( \sum_{l=1-N_f}^0 w_l h_{k-l} \right) \right\}^2 \\ & + E \left\{ \left[ \text{Re} \left( \sum_{l=1-N_f}^0 w_l n_{k-l} \right) \right]^2 \right\} = \\ & \sum_{k=1-N_f}^0 \sum_{l,m=1-N_f}^0 (w_l^r h_{k-l}^r - w_l^i h_{k-l}^i) (w_m^r n_{k-m}^r - w_m^i n_{k-m}^i) + \\ & E \left[ \sum_{l,m=1-N_f}^0 (w_l^r n_{k-l}^r - w_l^i n_{k-l}^i) (w_m^r n_{k-m}^r - w_m^i n_{k-m}^i) \right] = \\ & \sum_{l,m=1-N_f}^0 w_l^r w_m^r \left( \sum_{k=1-N_f}^0 h_{k-l}^r h_{k-m}^r + E[n_{k-l}^r n_{k-m}^r] \right) \\ & + \sum_{l,m=1-N_f}^0 w_l^r w_m^i \left( - \sum_{k=1-N_f}^0 h_{k-l}^r h_{k-m}^i + E[-n_{k-l}^r n_{k-m}^i] \right) + \\ & \sum_{l,m=1-N_f}^0 w_l^i w_m^r \left( - \sum_{k=1-N_f}^0 h_{k-l}^i h_{k-m}^r + E[-n_{k-l}^i n_{k-m}^r] \right) + \\ & \sum_{l,m=1-N_f}^0 w_l^i w_m^i \left( \sum_{k=1-N_f}^0 h_{k-l}^i h_{k-m}^i + E[n_{k-l}^i n_{k-m}^i] \right). \end{aligned} \quad (30)$$

We assume additive complex white Gaussian noise with equal and independent real and imaginary components, and we define an autocorrelation function  $R_{l-m} =$

$E[n_{k-m} n_{k-l}^*]$ . Deriving the real and imaginary parts of this function we arrive at

$$\begin{aligned} \frac{1}{2} R_{l-m}^r &= E[n_{k-m}^r n_{k-l}^r] = E[n_{k-m}^i n_{k-l}^i] \\ \frac{1}{2} R_{l-m}^i &= E[n_{k-m}^i n_{k-l}^r] = E[-n_{k-m}^r n_{k-l}^i] \end{aligned} \quad (31)$$

Let us define

$$\begin{aligned} \tilde{\Omega}_{2l,2m}^r &= \sum_{k=1-N_f}^0 h_{k-l}^r h_{k-m}^r + \frac{1}{2} R_{l-m}^r \\ \tilde{\Omega}_{2l,2m+1}^r &= - \sum_{k=1-N_f}^0 h_{k-l}^r h_{k-m}^i - \frac{1}{2} R_{l-m}^i \\ \tilde{\Omega}_{2l+1,2m}^r &= - \sum_{k=1-N_f}^0 h_{k-l}^i h_{k-m}^r + \frac{1}{2} R_{l-m}^i \\ \tilde{\Omega}_{2l+1,2m+1}^r &= \sum_{k=1-N_f}^0 h_{k-l}^i h_{k-m}^i + \frac{1}{2} R_{l-m}^r. \end{aligned} \quad (32)$$

Following a similar derivation we define the imaginary part of  $\tilde{\Omega}$

$$\begin{aligned} \tilde{\Omega}_{2l,2m}^i &= \sum_{k=1-N_f}^0 h_{k-l}^i h_{k-m}^i + \frac{1}{2} R_{l-m}^r \\ \tilde{\Omega}_{2l,2m+1}^i &= \sum_{k=1-N_f}^0 h_{k-l}^i h_{k-m}^r - \frac{1}{2} R_{l-m}^i \\ \tilde{\Omega}_{2l+1,2m}^i &= \sum_{k=1-N_f}^0 h_{k-l}^r h_{k-m}^i + \frac{1}{2} R_{l-m}^i \\ \tilde{\Omega}_{2l+1,2m+1}^i &= \sum_{k=1-N_f}^0 h_{k-l}^r h_{k-m}^r + \frac{1}{2} R_{l-m}^r. \end{aligned} \quad (33)$$

Combining the real and imaginary parts of  $\tilde{\Omega}$  we can write

$$\tilde{\Omega} = \tilde{\Omega}^r + \tilde{\Omega}^i. \quad (34)$$

Define  $\tilde{w}_{2k} = \text{Re}(w_k)$ ,  $\tilde{w}_{2k+1} = \text{Im}(w_k)$ ,  $\tilde{p}_{2k} = \text{Re}(p_k)$  and  $\tilde{p}_{2k+1} = \text{Im}(p_k)$ . Using the defined matrix  $\tilde{\Omega}$ , equations (30) and (31), we can write equation (28) in the following form:

$$\varepsilon_c^2 = \tilde{\mathbf{w}}^T \tilde{\Omega} \tilde{\mathbf{w}} - 2(\tilde{\mathbf{w}}^T \cdot \tilde{\mathbf{p}}) + 1 \quad (35)$$

In order to find the DFE equation for the BPSK case, we define as an optimization problem to bring the following MSE to minimum, where we ignore the imaginary ISI and noise and substitute  $\tilde{\Omega} = \tilde{\Omega}^r$  in equation (35)

$$\varepsilon_r^2 = \tilde{\mathbf{w}}^T \tilde{\mathbf{\Omega}}^r \tilde{\mathbf{w}} - 2(\tilde{\mathbf{w}}^T \cdot \tilde{\mathbf{p}}) + 1. \quad (36)$$

Taking the gradient of  $\varepsilon_r^2$  with respect to  $\tilde{\mathbf{w}}$  and setting it equal to zero we arrive at the equation

$$\tilde{\mathbf{w}} = (\tilde{\mathbf{\Omega}}^r)^{-1} \tilde{\mathbf{p}}, \quad (37)$$

from which the DFE coefficients are calculated.

In the partial precursor cancelling case we minimize only some of the imaginary precursors. Let  $-L$  be the index of the last imaginary precursor included in the minimization. This results in new definitions for  $\tilde{\mathbf{\Omega}}^i$  which are given by

$$\begin{aligned} \tilde{\Omega} p_{2l,2m}^i &= \sum_{k=1-N_f}^{-L} h_{k-l}^i h_{k-m}^i + \frac{1}{2} R_{l-m}^r \\ \tilde{\Omega} p_{2l,2m+1}^i &= \sum_{k=1-N_f}^{-L} h_{k-l}^i h_{k-m}^r - \frac{1}{2} R_{l-m}^i \\ \tilde{\Omega} p_{2l+1,2m}^i &= \sum_{k=1-N_f}^{-L} h_{k-l}^r h_{k-m}^i + \frac{1}{2} R_{l-m}^i \\ \tilde{\Omega} p_{2l+1,2m+1}^i &= \sum_{k=1-N_f}^{-L} h_{k-l}^r h_{k-m}^r + \frac{1}{2} R_{l-m}^r, \end{aligned} \quad (38)$$

where  $L \in 0, \dots, N_f$ . Now we have another optimization problem. We want to minimize both  $\varepsilon_r^2$  and  $\varepsilon_i^2$  (where  $\varepsilon_i^2$  is the error caused by the minimized imaginary ISI and noise), so we optimize  $\varepsilon_r^2 + \beta \varepsilon_i^2$  by substituting  $\tilde{\mathbf{\Omega}} = \tilde{\mathbf{\Omega}}^r + \beta \tilde{\mathbf{\Omega}}^i \mathbf{p}^i$  in equation (35), where  $\beta$  is a weight factor. We use  $\beta = 1$  (so that the real and imaginary parts have the same weight), and the DFE equation that minimizes the resulting MSE is given by

$$\tilde{\mathbf{w}} = (\tilde{\mathbf{\Omega}}^r + \tilde{\mathbf{\Omega}}^i \mathbf{p}^i)^{-1} \tilde{\mathbf{p}}. \quad (39)$$

where  $\tilde{\mathbf{\Omega}}^i \mathbf{p}^i$  is given in equation (38).

Manuscript received on April 30th, 1999.

## REFERENCES

- [1] R. Krishnamoorthy. "Equalization and Antenna Diversity for Indoor Radio Modem". In *Wireless Networks - Catching the Mobile Future*, 5<sup>th</sup> IEEE International Symposium on Personal, Indoor and Mobile Radio Communications (PIMRC), Vol. 4, pages 1373-1377, 1994.
- [2] J. Tellado-Mourello, E.K. Wesel, J.M. Cioffi. "Adaptive DFE for GMSK in Indoor Radio Channels". *IEEE J. Select. Areas Comm.*, Vol. 14, No. 3, pages 492-501, April 1996.
- [3] N.W.K. Lo, D.D. Falconer, A.U.H. Sheikh. "Adaptive Equalization for Co-Channel Interference in a Multipath Fading Environment". *IEEE Trans. Comm.*, Vol. 43, No. 2/3/4, pages 1441-1452, Feb.-April 1995.
- [4] D. Raphaeli. "Efficient DFE Initialization for High Speed Wireless LAN". In *ICUPC, Florence, Italy*, pages 717-720, 1998.
- [5] I. Lee, J.M. Cioffi. "A Fast Computation Algorithm for the Decision Feedback Equalizer". *IEEE Trans. Comm.*, Vol. 43, No. 11, pages 2742-2749, Nov. 1995.
- [6] L. Dossi. "Performance Analysis of GMSK Discriminator Integrator Detection with Decision Feedback Equalization in Land Mobile Radio Channel". In *Wireless Networks - Catching the Mobile Future*, 5<sup>th</sup> IEEE International Symposium on Personal, Indoor and Mobile Radio Communications (PIMRC), Vol. 4, pages 1317-1321, 1994.
- [7] T.K. Ohno, F. Adachi. "GMSK Frequency Detection Using Decision Feedback Equalization". *Electron. Lett.*, Vol. 23, No. 25, pages 1350-1351, Dec. 1987.
- [8] S.W. Wales. "Modulation and Equalization Techniques for HIPERLAN". In *Wireless Networks - Catching the Mobile Future*, 5<sup>th</sup> IEEE International Symposium on Personal, Indoor and Mobile Radio Communications (PIMRC), Vol. 3, pages 959-963, 1994.
- [9] A. Nix, M.Li, J. Marvill, T. Wilkinson, I. Johnson, S. Barton. "Modulation and Equalization Considerations for High Performance Radio LANs (HIPER-LAN)". In *Wireless Networks - Catching the Mobile Future*, 5<sup>th</sup> IEEE International Symposium on Personal, Indoor and Mobile Radio Communications (PIMRC), Vol. 3, pages 964-968, 1994.
- [10] G. Yang, K. Pahlavan, T.J. Holt. "Sector Antenna and DFE Modems for High Speed Indoor Radio Communications". *IEEE Trans. Veh. Technol.*, Vol. 43, No. 4, pages 925-933, Nov. 1994.
- [11] N. Al-Dhahir, J.M. Cioffi. "MMSE Decision-Feedback Equalizers: Finite-Length Results". *IEEE Trans. Inform. Theory*, Vol. 41, No. 4, pages 961-975, July 1995.
- [12] J.E. Smee and N.C. Beaulieu. "On the Equivalence of the Simultaneous and Separate MMSE Optimizations of a DFE FFF and FBF". *IEEE Trans. Comm.*, Vol. 45, No. 2, pages 156-158, Feb. 1997.

